Nuno Miguel Teixeira Coelho

Licenciado em Ciências de Engenharia de Micro e Nanotecnologias

Improving Silicon Probe Performance Through Layer-by-Layer Coating

Dissertação para obtenção do Grau de Mestre em
Engenharia de Micro e Nanotecnologias

Orientador: Adam Kampff, Professor Doutor,
Champalimaud Center for the Unknown

Co-orientadores: Elvira Fortunato, Professora Doutora,
Faculdade de Ciências e Tecnologia da Universidade Nova de Lisboa

FACULDADE DE CIÊNCIAS E TECNOLOGIA
UNIVERSIDADE NOVA DE LISBOA

Outubro, 2015

Improving Silicon Probe Performance Through Layer-by-Layer Coating

Faculdade de Ciências e Tecnologia da Universidade Nova de Lisboa

"Time you enjoy wasting, was not wasted" – John Lennon

Acknowledgements

What a harsh and also fun dissertation this was. For starters, I would like to thank everyone that made this huge step in my academic life possible. This project was achievable throughout 5 years of university in which fun, friendship, love, and work took part of, and it was all the people that I met and lived with that made those years so great. It's impossible to thank each person individually that helped me through these challenging and adventurous times, and I truly hope that no one will take it personally for not making it in to this (finite) text. That said, I would like to sincerely thank the following:

To Dr. Adam Kampff for the opportunity to work with a great group in the amazing institution that the Champalimaud Centre for the Unknown (CCU) is. It was an experiment that I will remember my whole life, and where I've grown academically and as a person as well. All the notes, comments and remarks given were extremely useful and enlightening, and allowed me to make a master thesis that I can be proud of.

To Dr. Elvira Fortunato, for all she was done for nanotechnology around the world and especially in our university, enabling the formation of hundreds of well prepared future engineers.

To Joana Neto for all she had to put up with me. Since my day one till the last day, she was there to guide and help me, and I can't thank her enough for the infinite patience. Without her, this project simply wouldn't be possible, and I think that that says it all.

To the rest of the group that constitutes the Intelligent Systems Lab at the CCU, for turning this experience in a fun and educational time: George Dimitriadis, Pedro Lacerda, João Frazão, Joana Nogueira and Gonçalo Lopes.

To Pedro Baião, who had no obligation whatsoever to help me, and yet he did. Much of my work was supported by his previous project, and without it, this master thesis would be far less interesting.

To Tiago Monteiro for all the help with the post-surgery recordings and explanations of how the all process works. Also a very special thanks to William, the mouse that took this thesis to a all new level.

To everyone at CENIMAT/I3N that helped me and contributed to the relaxed and amazing environment present there.

To the micro and nanopeople that supported me over the years and provided 5 years of great fun.

To all the good friends that accompanied me in the best years of my life (so far, hopefully!). To my friendship friends: Ana Castanho, André Castro, Francisco Nunes, Joana Cabral, Joana Nave, Maria João, Pedro Castanho, Pedro Palma and Rui Carreiras, for all the fun and stupid moments in school and in the innumerous coffees and night outs we had. To all my academic godchildren and grandchildren that made me proud over the years. To Constança Oliveira, Joana Almeida e Sofia Martins for all the patience and love, and for helping me be the men I am today (for better or worse!). Finally, last but not least, to my best friends over the years: Afonso Ferreira, Daniel Pereira, Diogo Vaz, João Jacinto, João Rosa, Júlio Costa, Moisés Tereso, Pedro Figueiredo and Tiago Rosado. All of us, one way or the other were part of the great and mythic place that Basolho became, and I wanted to thank you for all the parties and unforgettable moments that we shared over the years.

To my love ones, without whom I would be lost. To all my family, for all the Easters, birthdays and Christmas I spent among them. To my sister, for growing up with me and for teaching me, through a mist of funny and really stressful moments, what is love all about. Finally, I would like to thank to my mom and dad. All my life I looked up and though that my parents were heroes. Today, I'm sure they are, and I'm forever thankful for all the love they gave me.

Abstract

Fully comprehending brain function, as the scale of neural networks, will only be possible with the development of tools by micro and nanofabrication. Regarding specifically silicon microelectrodes arrays, a significant improvement in long-term performance of these implants is essential. This project aims to create a silicon microelectrode coating that provides high-quality electrical recordings, while limiting the inflammatory response of chronic implants.

To this purpose, a combined chitosan and gold nanoparticles coating was produced allied with electrodes modification by electrodeposition with PEDOT/PSS in order to reduce the impedance at 1kHz. Using a dip-coating mechanism, the silicon probe was coated and then characterized both morphologically and electrochemically, with focus on the stability of post-surgery performance in anesthetized rodents. Since not only the inflammatory response analysis is vital, the electrodes recording degradation over time was also studied.

The produced film presented a thickness of approximately 50 μm that led to an increase of impedance of less than 20 kΩ in average. On a 3 week chronic implant, the impedance increase on the coated probe was of 641 kΩ, compared with 2.4 MΩ obtained for the uncoated probe. The inflammatory response was also significantly reduced due to the biocompatible film as proved by histological tests.

Keywords: neurons, microelectrodes, biocompatibility, impedance, layer-by-layer

Resumo

De modo a compreender totalmente o funcionamento do cérebro, especialmente no que à comunicação entre os neurónios diz respeito, o desenvolvimento da micro e nanofabricação é essencial. Analisando especificamente matrizes de microeléctrodos de silício, verifica-se que o seu desempenho em implantes de longo período é ainda deficitário. Este projecto tem como objectivo a criação de um revestimento biocompatível para essas mesmas matrizes de modo a proporcionar a obtenção de sinais eléctricos sem diminuição da sua qualidade, bem como minimizar ao máximo a resposta inflamatória por parte do organismo.

Para este efeito, um revestimento combinado de quitosano e nanopartículas de ouro foi criado, aliado à modificação prévia dos microeléctrodos através da electrodeposição de PEDOT/PSS, de modo a reduzir a sua impedância a 1 kHz. Recorrendo a um mecanismo de imersão por camadas, o filme foi depositado sobre a sonda de silício sendo depois caracterizada morfológica e electroquimicamente, com especial foco no desempenho em implantes crónicos. Tanto o nível de resposta inflamatória como a degradação do sinal eléctrico obtido ao longo do tempo por parte dos microeléctrodos foram estudados.

O filme produzido, com cerca 50 nm leva a um aumento na magnitude da impedância de menos de 20 kΩ e posteriormente permite que um implante após 3 semanas apresente um aumento de cerca de 641 kΩ, ao invés de 2.4 MΩ num implante sem a presença do filme biocompatível de quitosano e nanopartículas de ouro. A presença do filme originou também uma redução da resposta inflamatória por parte do organismo.

Palavras-chave: neurónios, microeléctrodos, biocompatibilidade, impedância, camada por camada

Abbreviations

AFM	Atomic Force Microscope
Ag	Silver
AgCl	Silver Chloride
Au	Gold
AuNp's	Gold Nanoparticles
Chi	Chitosan
DLS	Dynamic Light Scattering
EEG	Elecroencephalography
F-MRI	Functional Magnetic Resonance Imaging
LFP	Local Field Potential
O	Oxygen
PBS	Phosphate-buffered Saline
PEDOT	Poly(3,4-ethylenedioxythiophene)
PET	Positron Emission Tomography
PPy	Poly(pyrrole)
PSS	Poly(styrenesulfonate)
SEM	Scanning Electron Microscope
Si	Silicon

Table of contents

Figure Index

Table Index

1. Introduction

The pursuit of the unknown is what keeps researchers going forward, evolving at each step. Understanding how the brain works, learning and understanding all the functionalities of it would allow us to better comprehend our behaviors and personalities, as well as to extend our well-being and health. The treatment and perhaps the cure of several pathologies such as strokes, sensory deficits, or neurological diseases, such as Epilepsy, Parkinson's or even Alzheimer's would then be possible [1]. That said, it is clear that through science and engineering, a full comprehension of the human and animal neural system has yet to be achieved.

To explore the vast neuron network that constitutes the nervous system (with over 85 billion neurons), invasive and non-invasive techniques can be used. Positron emission tomography (PET), single-photon-emission computer tomography (SPECT), electroencephalography (EEG) or functional magnetic resonance imaging (f-MRI) provide an image of the brain's anatomy, however with a poor spatial and/or temporal resolution [2]. To actually detect neurons activity and their vast network invasive tools are usually required [3]. Over the years, micro and nanofabrication development led to the improvement of neural probes, with an increasing number of recording electrodes, as well as a decrease in its overall dimensions (Figure 3). From microwires [4], to silicon micro machined probes [5], polymers substrates (flexible) [6], or even stimulation of specific proteins using optical fiber [7], a vast range of different invasive recording techniques are now available, enabling high spatio-temporal resolution that led to a significantly progress in basic neuroscience comprehension [2]. Some examples of neural probes are depicted in Figure 1.

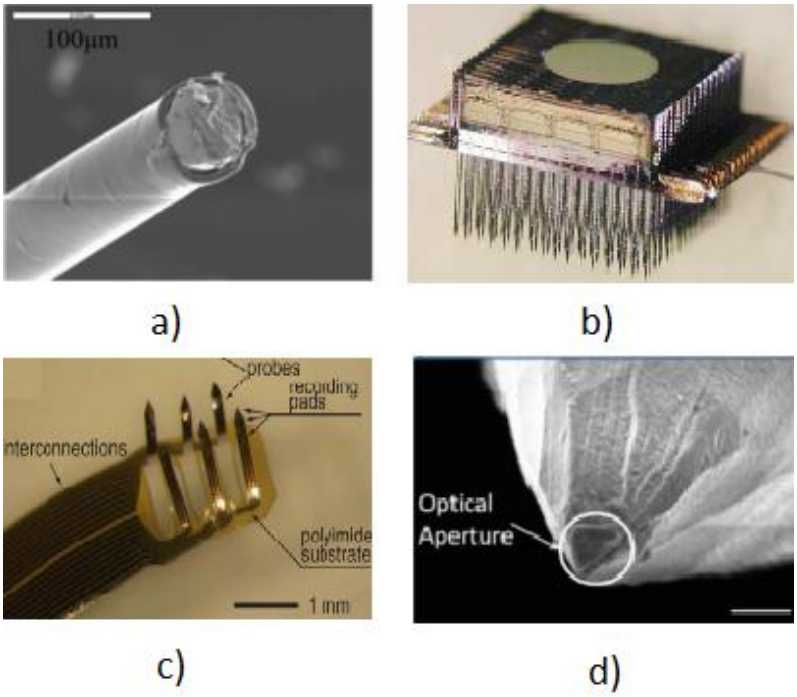

Figure 1 - Various systems configurations for neural study. Single tungsten wire without modifications (a) [8]**; Michigan probe, a silicon based neural probe with 1024 electrodes (b); Flexible probe array constituted by polyimide (c)** [9]**; Single optrode, with both recording and stimulation function. Light is then delivered through the fiber, reaching the nearby neurons (d)** [7]**.**

But what do we aim to measure specifically? Usually in a cell the interior's potential is negative when compared with the exterior, leading to a voltage difference, or resting membrane potential. However, when the potential inside the cell temporally becomes positive, due to diffusion of ions through the membrane, an action potential is generated [10]. By placing extracellular electrodes in the brain, those action potentials can be detected [11]. The measured signal is the sum of numerous electrical sources (neurons) from the brain tissue, so a signal containing all the extracellular activity close to the electrode is obtained, being necessary a posterior analysis to isolate and determine the neurons activity (Figure 2). As the distance between the conducting electrode and the neurons increases, less information regarding the selected area is gathered. Thereby, a tight seal between the neuron and the electrode is essential, so that along with a reduced inflammatory response, a high spatial resolution is obtained [12]. Usually the maximum distance between the microelectrode and the nearby neurons recorded is approximately 50-100µm. [13] The main goal is to record and isolate the maximum number of neurons and at the same time to keep the implanted electrodes for the longest period of time possible.

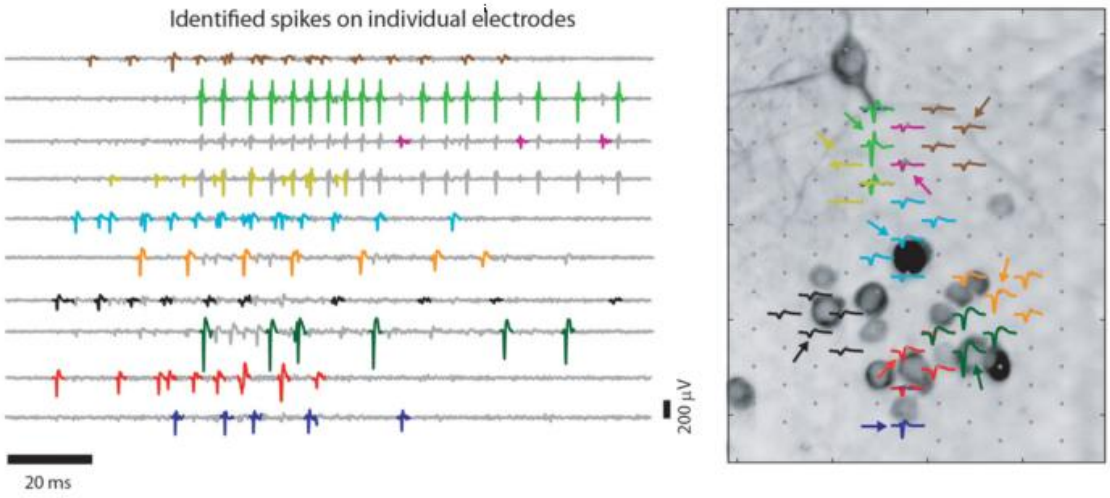

Figure 2 – Spikes detected for 10 different neurons (left) and the location where they were measured (right). Different electrodes can measure the same signal, where the electrode with the highest peak-to-peak amplitude is chosen to be analyzed. [14]

There are still some challenges regarding the use of implantable microelectrode, especially concerning signal-to-noise ratio values and long-term stability [1]. Higher electrode impedance leads to inferior signal-to-noise ratio, contrary to what is desired for an enhanced quality recording. PEDOT (Poly 3,4-ethylenedioxythiophene) is a conducting polymer that's been used in recent years, showing promising results in experiences of neural implants *in vitro* [15] [16] and *in vivo* [17]. PEDOT is commonly combined with PSS (Poly (styrenesulfonate)), as in this thesis. The electrodeposition of PEDOT:PSS leads to a lower impedance at 1kHz (to match the frequency of the average neuron spike), improving as well the electrodes performance over an extended period of time.

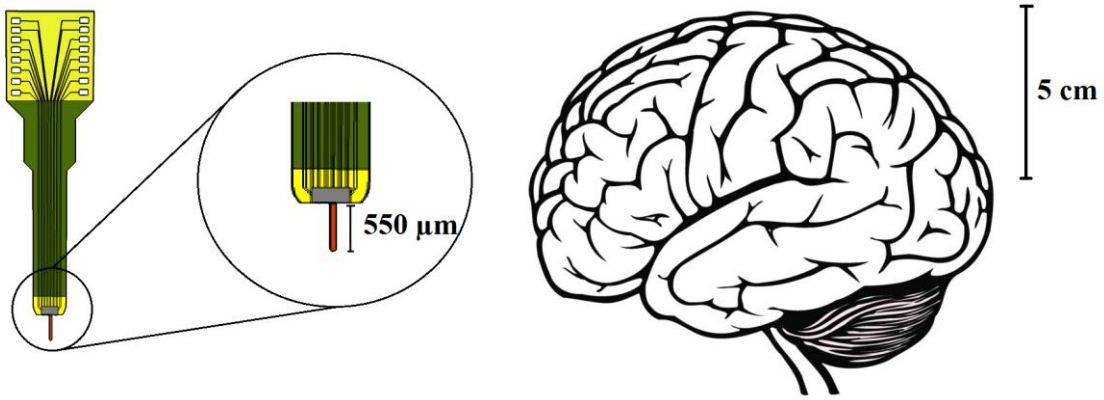

Figure 3 – Invasive probe dimensions compared with a human brain (usually the final depth of the implant is only of a few millimeters). Despite the probe's size is significantly minute compared to our brain, the scar formation is an issue that needs to be tended for long term implants.

In neural electrodes implants, the impedance in electrode-electrolyte interface could be affected by several factors, such as electrode micromotion and bacterial growth [18]. Although the biological processes are still not fully understood, brain tissue reaction is considered the main cause of neural implants malfunction, making it the primary concern in neural implants design [4]. After the probe's insertion, an immune inflammatory response takes place, characterized by the migration and proliferation of glial cells such as astrocytes and microglia. The presence and action of these cells leads to an inevitable scar formation around the probe, isolating it from the remain tissue and increasing the electrodes impedance [19]. Despite the immediate inflammatory response, the electrodes recordings remain virtually unaffected, however for chronic implants, the immune response effects tend to make the device unusable. [20]

This gliar scar formation can be minimized by the coating of biocompatible materials covering the entire probe surface or each electrode individually (or both, as suggested in this thesis), leading also to a higher charge storage capacity, that is, the increase of the maximum charge that can be injected without causing irreversible faradic reactions. [15]

For this thesis, a combined coating of chitosan and gold nanoparticles was chosen, along with an microelectrode modification with PEDOT:PSS (Figure 4).

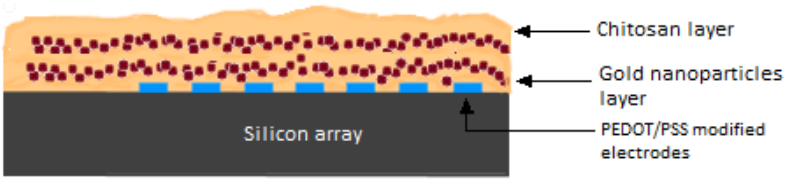

Figure 4 – Representation of the structural modifications on silicon microelectrode arrays. The process begins with the electrodes modification with PEDOT/PSS, followed by layer-by-layer coating with chitosan and gold nanoparticles.

Chitosan is a natural polysaccharide obtained by treatment of crustacean shells, and it is frequently used in neuroscience (mainly in drug delivery) due to its biocompatibility, anti-inflammatory properties and also an adhesion ability [21] [22]. A enhanced attachment and cells growth is also favored by the chitosan cationic amine groups [23]. Also, despite some controversy on the use of nanoparticles in tests and treatments in the human organism, gold nanoparticles are already used in medical practice with a proven reduced toxicity [24]. Nanoparticles can be used with the purpose of providing a higher adhesion between polymers and biological tissue, or even between polymers only, which can lead to an effective reduction in the film total thickness. The adhesive property is fundamental in reducing the inflammatory response due to the decreasing distance between neurons and the electrode, leading to a more "friendly" assem-

bling between the silicon probe and the extracellular mean [25]. Since the neurons “reaction” to the implanted probe is improved by the contact with rough surfaces, the deposition of nanoparticles lead to a higher thickness of the film.

2. Materials and Methods

The experimental work evolved the preparation of several solutions and layer-by-layer and electrodeposition techniques to obtain the structural changes in the silicon probes. Posterior, morphological, electrochemical and *in vivo* characterizations were performed. In this chapter, all the solutions and techniques employed are explicit.

2.1 Solution-based synthesis

2.1.1 Chitosan

Chitosan composite (>75% deacetylation) was obtain from Santa Cruz Biotechnology. Chitosan solution (1% w/w) was prepared mixing distilled water with acetic acid (1% v/v).

2.1.2 Gold nanoparticles (AuNp's)

The citrate reduction method was used to synthesize of gold nanoparticles. A solution consisting of 1 mM of tetrachloroauric acid (Sigma-Aldrich, 99.9%) was heated on a hot plate with a magnetic stirrer until it reached the boiling point. To this solution, 1% (w/v) trisodium citrate (AnalaR NORMAPUR, 100%) was added and continuously stired. The solution was removed after it turn red from the hot plate. [26]

2.1.3 Poly(3,4-ethylenedioxythiophene) – Poly(styrenesulfonate) (PEDOT:PSS)

Synthesis of EDOT:PSS is obtained my mixing 0.01 M of EDOT (Sigma-Aldrich, 97%, M_W = 142.18) in water and then add 0.1 M of PSS (Sigma-Aldrich, M_W = 1000000), while stirred till the complete dissolution of EDOT.

2.2 AuNp's Characterization

2.2.1 Dynamic Light Scattering (DLS)

Hydrodynamic diameter of gold nanoparticles in water was confirmed by Dynamic Light Scattering (DLS) technique (W130i Avid Nano).

2.3 Coatings Characterization

2.3.1 Atomic Force Microscope (AFM)

Chitosan/AuNp coating morphology was analyzed by atomic force microscopy (AFM, Asylum Research MFP-3D Standalone).

2.3.2 Scanning Electron Microscopy (SEM)

Chitosan/AuNp coating morphology was confirmed by scanning electron microscopy (SEM-FIB, Zeiss Auriga).

2.3.3 Contact Angle

The hydrophilicity of the Chi/AuNp coating was tested using Contact Angle System OCA (Data Physics).

2.4 Silicon Probes

Different silicon probes with distinct configurations were used:

- One shank: 32 iridium electrodes with a diameter of 15µm.
- Eight shanks: 4 iridium electrodes per shank - 32 in total – with a 20µm diameter**.**

Additionally, silicon wafers were used and pieces of 1 x 2 cm were used for purposes of coating's degradation over time.

2.4.1 Dip-coating

The silicon probes coating was prepared using the layer-by-layer method. The probe is dipped in a constant speed in chitosan or in a gold nanoparticles solution, then removed and rinsed with distilled water and dried (Figure 4). The process is then repeated till the desired number of layers is achieved. The first and last layers are constituted by chitosan.

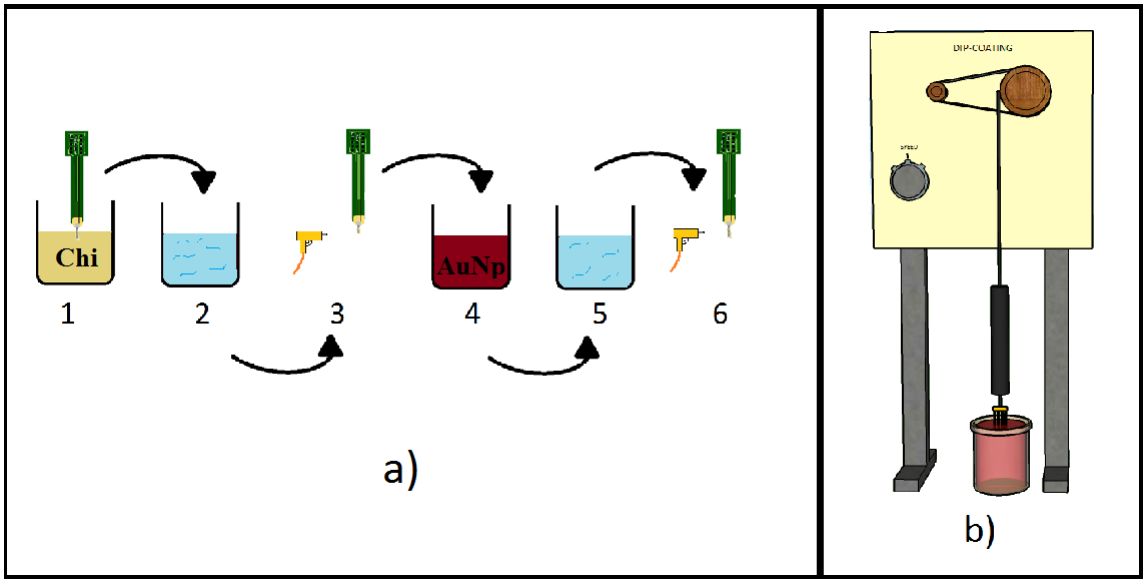

Figure 5 – Dip-coating procedure. Schematics of the different steps that constitute the process: 1,4 – chitosan and gold nanoparticles solution; 2,5 – distilled water; 3,6 – nitrogen drying (a); Dip-coating mechanism representation (b).

2.4.2 Impedance characterization

A NanoZ (Neuralynx) system with two electrode cell configuration was used to measure the electrodes impedance at 1 kHz. The different probes were connected as working electrodes, whereas an Ag/AgCl wire (Science Products GmbH, E-255) was the reference electrode.

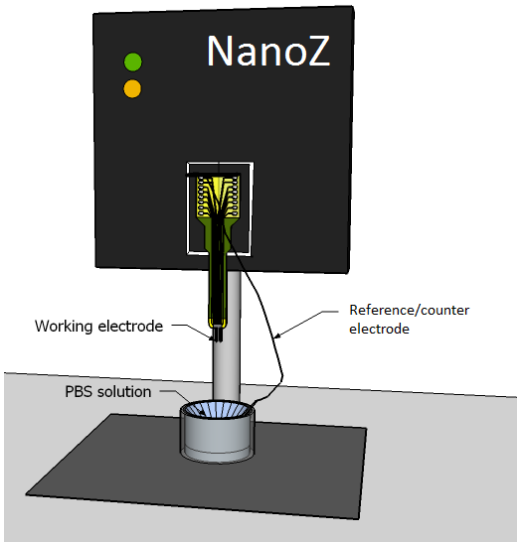

Figure 6 - Schematics of the NanoZ two electrode cell system configuration. The Ag/AgCl wire is used as reference and it is located around the cup while in contact with the solution, whereas the probe is positioned in the middle of the deposition cup, at an equal distance of the wire.

2.4.3 Morphological Characterization

Study of electrode structural modifications and coating was done by SEM (SEM-FIB, Zeiss Auriga) between 1 and 2 kV using a specific probe setup.

2.4.4 Electrodeposition Set-up

The PEDOT/PSS electrochemical depositions were performed using the NanoZ system represented in Figure 5. A galvanostatic deposition process was used, where the previous chosen current is remained constant over time. The deposition is made targeting each electrode individually, thanks to the software's 'Manual Control'.

2.5 Chronic Surgery

To analyze the coating's performance *in vivo* an anesthetized male rodent *(Long Evans)* with about 500g was used. During the surgery the rodent was immobilized and receiving anesthetic isoflurane (1 L/min O_2, 2% isoflurane), while the body temperature was constantly measured.

The surgical procedure has its beginning with the rodent's skin removal, leaving the targeted brain areas exposed. Then, using a rat brain atlas, the different landmarks on the skull are identified, proceeded by two craniotomies (4 x 2 mm, one for each probe) and the consequent dura matter removal.

Two high density electrode silicon arrays (Poly3-25s, Neuronexus Technologies) were inserted via a micromanipulator that descends at a constant speed (1 µm/s). The probes (one with Chi/AuNp's coating and one control) were located in the brain's frontal lobe on both hemispheres, with an equal distance to its middle.

2.6 *In vivo* Recordings

After one week from the surgery day the animal was connected to the recording system and the impedance and the signal were measured during 3 weeks for the 64 electrodes. The data was recorded using an open-source electrophysiology acquisition board (Open Ephys) along with a RDH2000 series digital electrophysiology interface chip. This chip had the function of filter, amplify and multiplex all the 64 channels (Intan Technologies). The electrodes are connected to one side of the chip, whereas digital data streams out the other side after analog-to-digital conversion (16-bit resolution).

2.7 Histological Characterization

Posterior to the chronic surgery, the brain was removed and cross sections in PBS 1x with 100mm thickness were made, being left to rest overnight. Hematoxylin and eosin staining procedure was then used to stain the cells nuclei and cytoplasm. The process begins with rinsing the samples with distilled water. ST HemalastTM (3801698B, 30 s) and ST Hematolxylin (3801698A, 3 min) were then applied. ST Differentiator™ (3801698C, 45 s) and ST Bluing Agent™ (3801698E, 1 min) were used next, with water rinsing between them. After that, ST Eosin™ (3801698D, 50 s) was applied, with alcohol at 96ºC for 1 min used before and after. Finally, Xilol solution was used for 3 min, with the posterior slides assembling with Entellan ® (Merck – HX135668). The samples were then observed with an optic microscope.

3. Results

3.1 Coating Characterization

3.1.1 Pre-Surgery Impedance Characterization

In order to define the ideal number of total layers for the film, an impedance test comparing the electrodes impedance values between five layers and eleven layers total was carried out in two silicon probes with 32 electrodes. The five layers and eleven layers had three and six chitosan layers coated, respectively, with gold nanoparticles deposited in between. In Figure 7, it's possible to observe a slightly increase in the impedance value for both probes, where the probe coated with five layers film experienced an impedance variation of around 12 kΩ (compared with 101 kΩ for the eleven layers probe – Table 1).

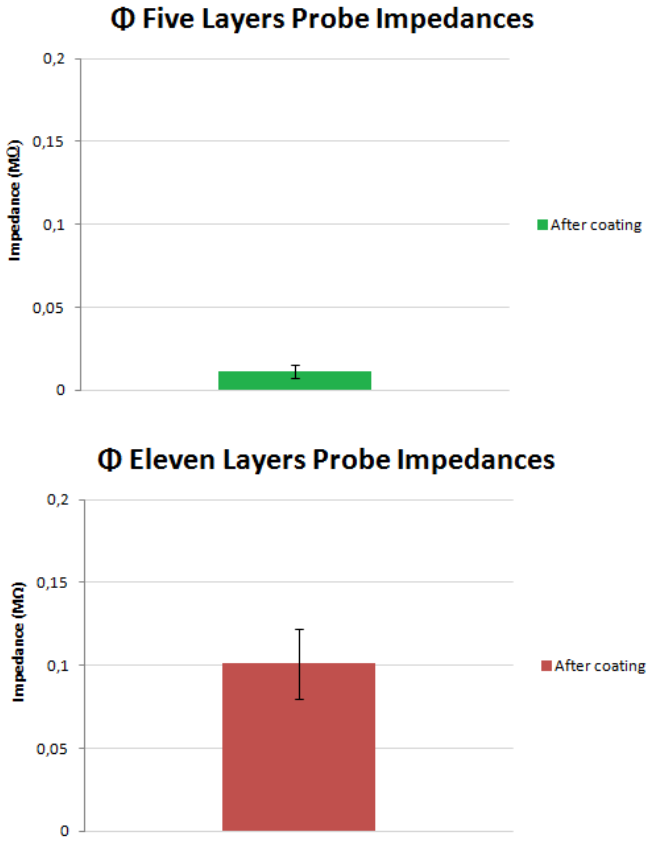

Figure 7 – Impedance variation after the deposition of the film for both probes. The probe coated with eleven layers total experienced a higher average impedance increase.

Table 1 – Average electrodes impedances and standard deviations for the probe with five and eleven layers coated.

	Five layers film	Eleven layers film
Impedance Variation (kΩ) ± SD (σ)	**11 ± 4**	**101 ± 22**

3.1.2 Morphologic Characterization

Coating's morphology was analyzed via SEM and AFM. To compare the film's thickness and roughness dependent on the number of layers coated, two silicon wafers were prepared with five and eleven layers in total. As expected, the silicon wafer coating with more layers deposited presented a superior thickness (200 nm, versus 40 nm, using ImageJ software), being also possible to observe a smoother surface compared with sample a) (Figure 8). The five layers total film provides then higher roughness, associated with a lower impedance magnitude, and so it was the film deposited for the chronic implanted probe. In figure 9 it is possible to observe the probe's coating with five layers where a homogenous film that covers all the electrodes is presented. This indicates the film's good adhesion to the silicon probe. It is also presented the gold nanoparticles diameter measured by DLS and SEM (using ImageJ – Table 2). The film's color was manually modified, as in the following images.

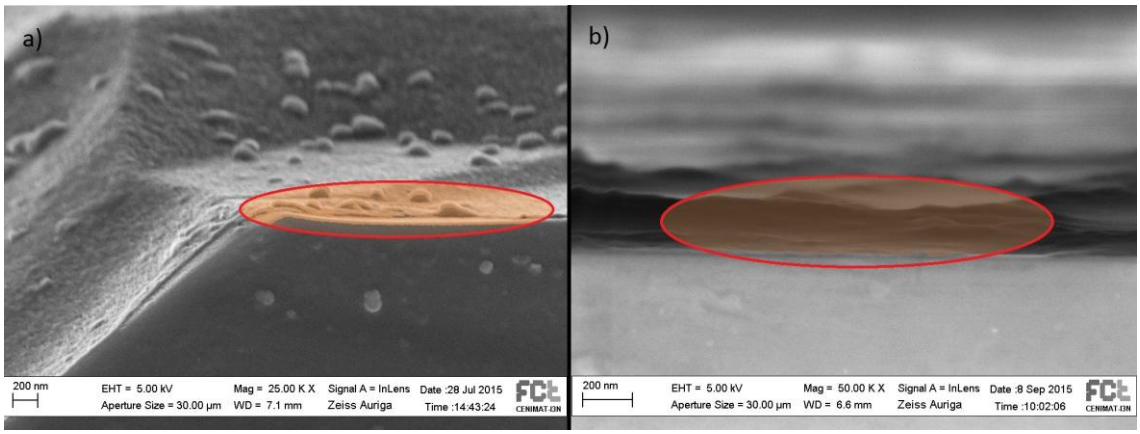

Figure 8 - Comparison between the two chitosan/gold nanoparticles films observed in SEM (highlighted in red): total of 5 layers – 40 nm (a); total of 11 layers – 200 nm (b).

Table 2 – Average AuNp's diameter and standard deviation by DLS and SEM.

DLS diameter (nm)	SEM nanoparticles diameter (nm)
16.4 ± 0.7	18.1 ± 2.9

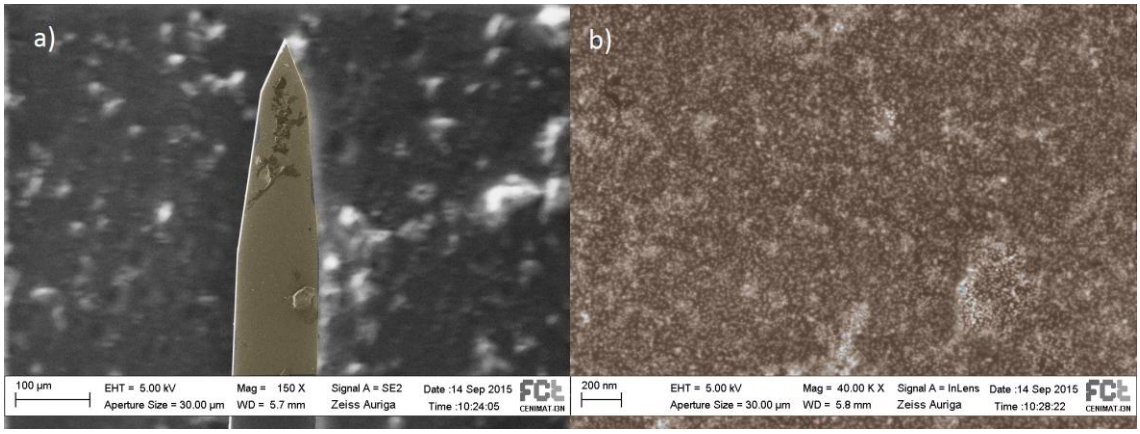

Figure 9 – Silicon probe with chitosan/AuNp coating observed in SEM showing some dust particles (a) and also some gold nanoparticles agglomerates (b).

In Figure 10, a more detailed study on the concentration of gold nanoparticles solution was carried out. For this study, AuNp's solution was centrifuged for 30 min at 9000 rpm. The supernatant was then removed and the remaining solution was used for silicon wafer coating (Figure 10 b), compared with the standard AuNp's solution used in Figure 10 a). It's possible to conclude that the average diameter of the structures formed by the gold nanoparticles is inferior in (a). This may be due to the higher concentration of nanoparticles, which tend to agglomerate in order to minimize the energy, whereas in (a) the nanoparticles are more dispersed. Despite the homogeneity in both solutions, the film in (a) presents more promising results compared with (b), due to a higher surface area and the inferior concentration of the solution used, leading to a smaller chance of nanoparticles released in the organism.

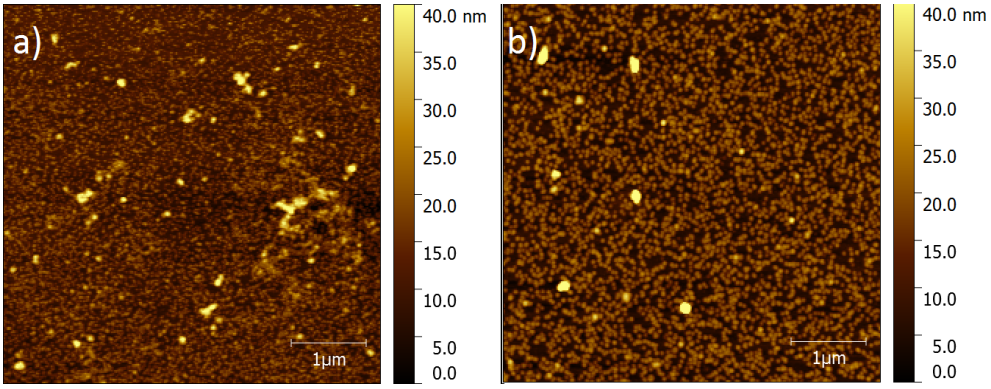

Figure 10 - Coating morphology study via AFM. Both films have the same number of layers deposited, although in b) the gold nanoparticles solution used had a higher concentration compared to the one in a).

3.1.3 Contact Angle

In Figure 11, we can see the shape of a PBS drop in a silicon wafer with the Chi/AuNp five layers film coated, with a contact angle of 64.7 ± 2.1º for both sides of the drop (below 90º the solution is considered hydrophilic), which is close to the ones obtained in the literature [23]. The roughness and hydrophilic properties promote an enhanced adhesion between the coating and the surrounding cells. The contact angle obtained for an uncoated silicon surface was of 59.2 ± 1.2º.

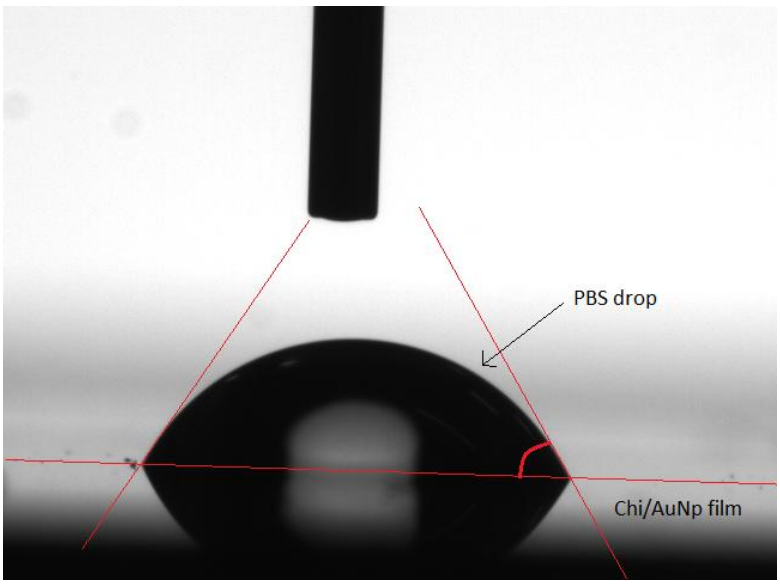

Figure 11 – Measurement of contact angle of a PBS drop in contact with Chi/AuNp coating.

3.1.4 Degradation Characterization

To test and analyze the 5 layers coating's degradation over time, in order to foresee the probe's performance in chronic implants, 2 different silicon wafers were placed inside a PBS solution (simulating the brain's conditions) at 37 ºC over a month, being one removed after two weeks and the other one after four weeks. Another silicon wafer was left out with the purpose of serving as a reference. Via SEM, it's possible to see that the coating's thickness slowly decreases over time, with the last silicon wafer coating having approximately one third the thickness (≈16 nm) of the control one (≈45 nm). That said, we can conclude that the coating resists in simulated brain conditions over a month, despite the reduction in thickness, and so the biocompatibility feature is expected to remain intact.

Table 3 - Average thickness obtained by SEM for the coating over a period of a month in PBS at 37 ºC.

SEM thickness (nm)		
Control	**2 Weeks**	**4 Weeks**
≈ 45	**≈ 22**	**≈ 16**

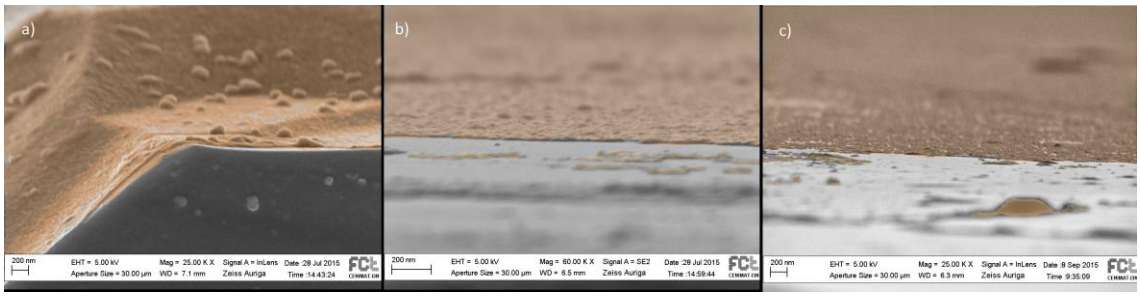

Figure 12 - Degradation of the chitosan/gold nanoparticles coating on a 37 ºC PBS solution over time. First, the control silicon wafer a); coating after two weeks b); coating after four weeks c).

3.1.5 Endurance Test

To evaluate the coating's mechanical resistance when penetrating the brain, a test with agar (a jelly-like substance derived from the polysaccharide agarose) was performed. The probe was inserted in agar (2% concentration) at a constant speed, and the impedances measured before and after were compared to analyze the coating's mechanical resistance (Figure 13). Following the five layers coating's deposition, the electrodes impedance values rose in an average of 102 kΩ (electrodeposition of PEDOT/PSS was not performed for this test probe, only the deposition of the film). This value is slightly superior to the one obtained before (12 kΩ). After the endurance test, not all the electrodes had the same behavior, but in average the electrode impedance increased around 38 kΩ, which indirectly proves that the coating remained attached to the probe, otherwise the final average impedance would be inferior to the one obtained. The rise in

impedance can then be explained with remains of agar still attached to the probe, despite the rinsing that was carried out.

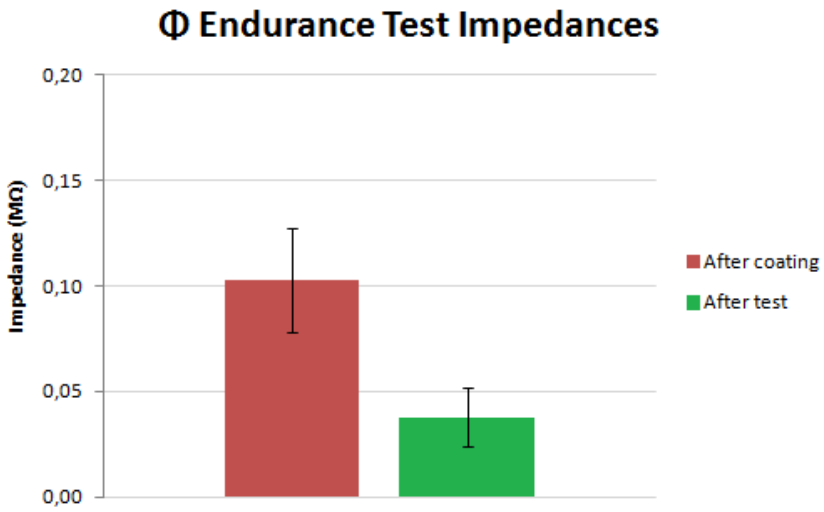

Figure 13 – Variation of the average impedance magnitude for 28 electrodes (at 1 kHz) after coating deposition (red) and after endurance test with agar (green).

3.2 *In vivo* Recordings

In chronic surgery we aimed to evaluate the performance differences between an uncoated and a coated silicon probe, both with respect to level of inflammatory response and quality of the recording signal. For that purpose, two silicon microelectrode arrays probes were inserted in a rodent's brain, both modified with PEDOT:PSS but only one with chitosan/AuNp film coating. Due to the imminent fall of the implants, there was need for an early perfusion of the rodent, and so the duration of the experiment was of three weeks instead of the four initially planned.

3.2.1. Electrodes Impedances

In Figure 14 is possible to observe for both probes that after the PEDOT:PSS electrodeposition all the electrodes impedance is significantly inferior (426 ± 100 kΩ and 152 ± 25 kΩ - uncoated and coated probe, respectively), enabling a possible significant improvement in neural recordings. Regarding the coated probe (five layers), an average rise of 7 kΩ was registered after the coating's deposition. On the second probe, only 25 electrodes had initial impedance lower than 2 MΩ (generally the electrical impedance limit for recording), instead of the original 32. This is due to earlier uses of the probes in other works, presenting varied initial impedance values for the electrodes, however, plenty electrodes remained active and able to record extracellular signals. For both probes, the final average impedance was around 100 kΩ.

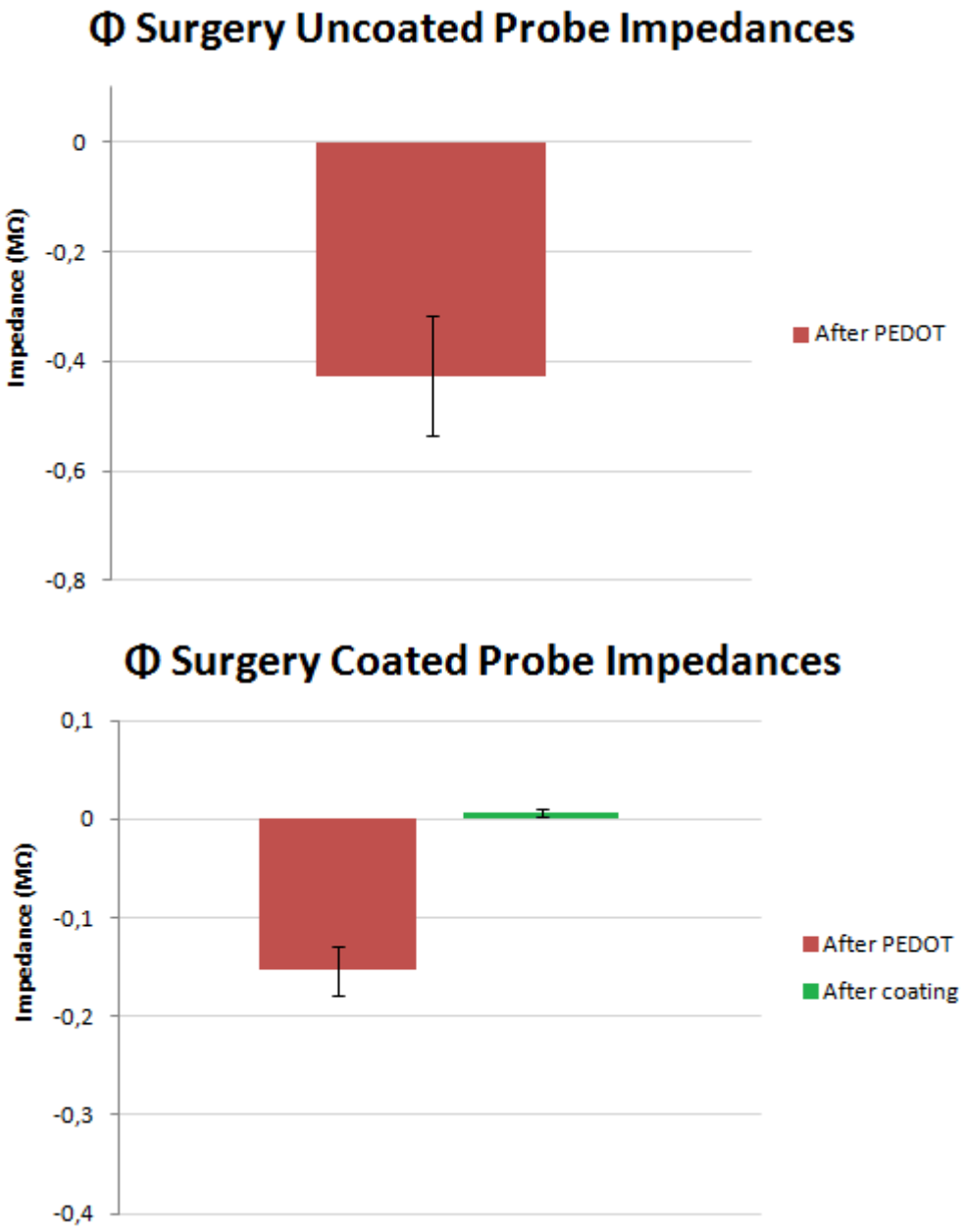

Figure 14 - Variation of the average impedance magnitude (at 1kHz) for the two chronic surgery selected probes. Impedances for probe 1, before and after the electrodeposition of PEDOT:PSS (a); Results obtained before and after PEDOT:PSS, and also after the deposition of the chitosan/AuNp coating (b).

In Figure 15, the average electrode impedance variation for the uncoated probe was of 1.159 ± 0.4 MΩ for the first week, 0.933 ± 0.2 MΩ for the second and 0.789 ± 0.12 MΩ during the third week. The coated probe presented a better performance in chronic implants than the uncoated one, as we can see in Figure 16. The impedance variation obtained were the follow: 0.340 ± 0.1 MΩ (week 1), 0.09 ± 0.03 MΩ (week 2) and 0.119 ± 0.03 MΩ (week 3).

The impedance variation for the probe coated with the Chi/AuNp film is then significantly inferior to the ones obtained for the uncoated probe, presenting strong evidence that the coating provided a biocompatible tissue that led to a reduction of the organism inflammatory response. This evidence is also supported by the detection of numerous and regular neuron spikes by the coated probe (results that together with the histology tests will be presented further on in this work). Relying in previous recording experiments performed on lab, electrodes with impedances above 2MΩ implied low signal to noise ratio being hard to detect spikes. Due to the inflammatory response already discussed, there was an increase in the electrodes impedances in both implanted probes, with the uncoated probe presenting a significant increase compared with the coated probe (this led to the inability to detect any neuron spiking activity with the uncoated probe, as it is demonstrated further on). The measured impedances experienced an increase over the three weeks experiment [27]. This can be explained by the agglomeration of immune system cells around the probes, leading to a further detachment between the recording electrodes and the nearby neurons.

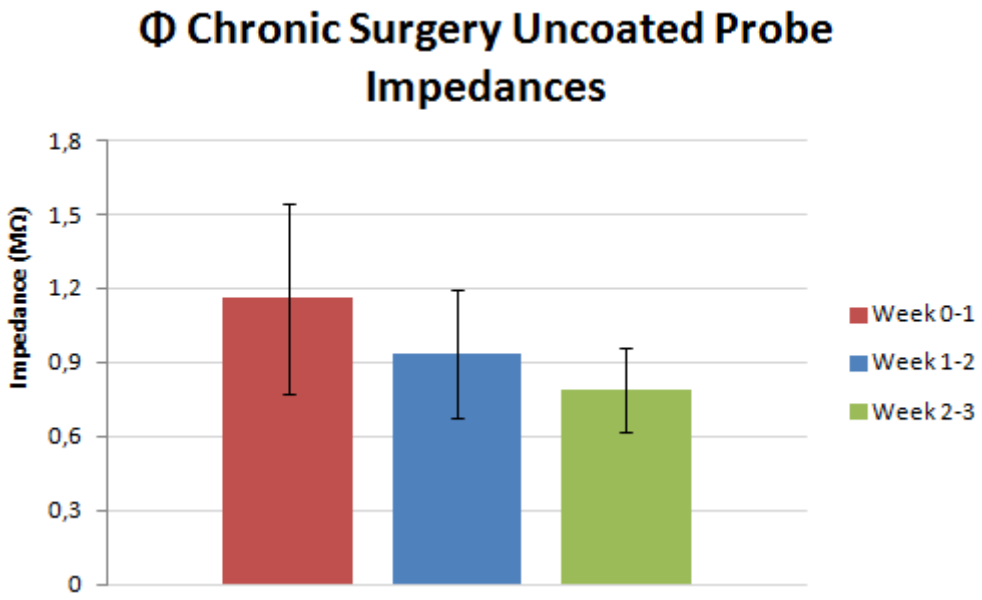

Figure 15 – Impedance variation on the uncoated probe throughout the chronic surgery. The impedances rose from each week to another, achieving an average maximum of 2,538 MΩ on the experiment's final week.

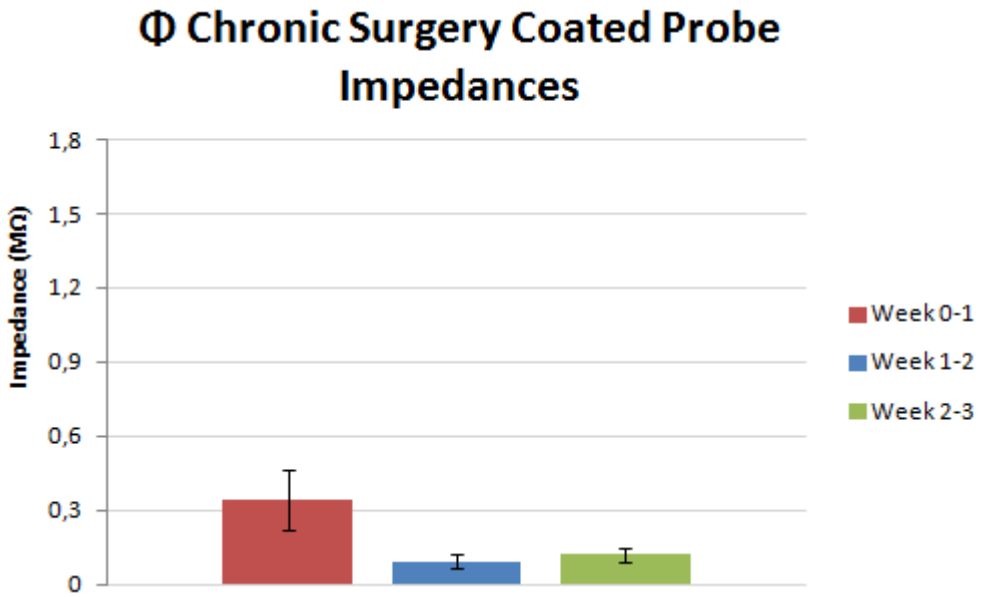

Figure 16 – Electrodes impedance variation for the coated probe, with a peak of 0.74 ± 0.4 MΩ at the end of the experiment.

3.2.2. Neurons Spikes

Throughout the chronic implantation, the rodent was connected to the acquisition board and the neurons spikes captured by the electrodes were measured and analyzed. To compare the performance between both probes, a single electrode (number 22) was chosen and the spikes detected were examined in terms of number of spikes and their average amplitude (Figure 17).

On the acute recordings (a and b), both probes detected several and ample neuron spikes, with an average amplitude of 314 µV and 418 µV for the uncoated and the coated probe, respectively. Half-way through the experiment (day 11 – c and d), some difference are already visible on the performance of both probes, not much in term of average amplitude (305 µV against 338 µV), but especially in the number of neuron single spikes detected, where the coated probe detected a much higher significant number when compared to the uncoated one. At the terminus of the experiment (e and f), the disparity between both probes performance is clearly evident. Due to the substantial increase in the electrodes impedance on the uncoated probe (as seen in Figure 15), the probe was unable to detect any neuron spikes, whereas the coated probe continued its neuron spikes detection with an average amplitude of 281 µV.

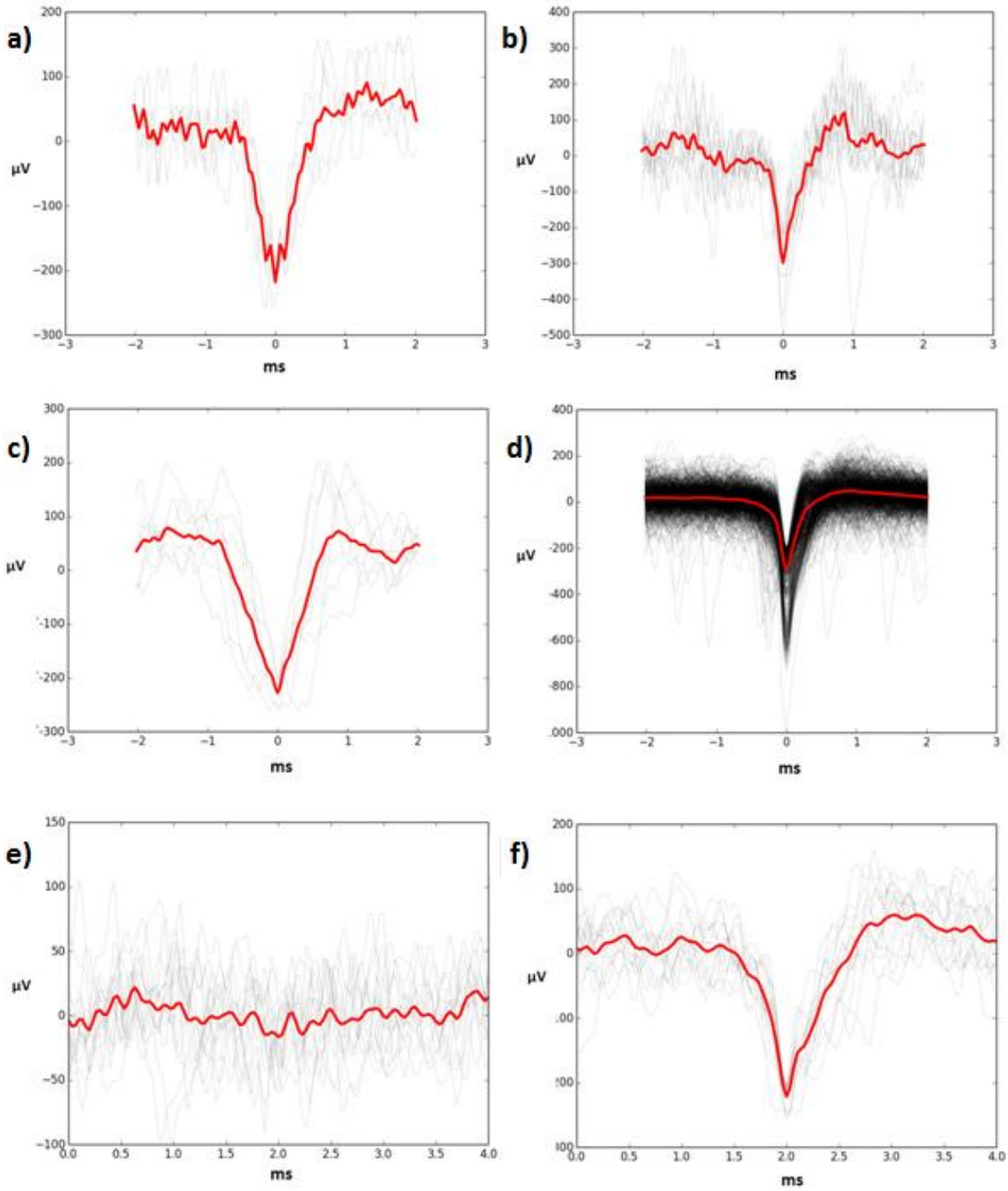

Figure 17 – Neuron spikes measuring and their average amplitude for the same electrode for both probes during the experiment at: day 0 – a) and b); day 11 – c) and d) and day 21 – e) and f). The uncoated probe is represented on the left (a, c and e) and the coated probe on the right of the figure (b, d and f).

3.2.3. Biocompatibility Characterization

To evaluate the organism inflammatory response, a conventional histology by hematoxylin and eosin staining of the rodent brain slices was carried out. The H&E staining enabled the visualization and differentiation of the diverse cells that constitute the immune response, allowing a comparison between the wounds caused by the implant of both probes.

After three weeks, the acute immune reaction already took place and it is followed by a chronic inflammatory response, characterized by the presence of glial cells such as lymphocytes and plasmocytes around the implants lesions (marked in Figure X). It is visible the superior number of these cells around the lesion caused by the uncoated probe when compared to the coated one, and so it is possible to conclude that the deposition of the biocompatible film lead to a reduced inflammatory response by the organism.

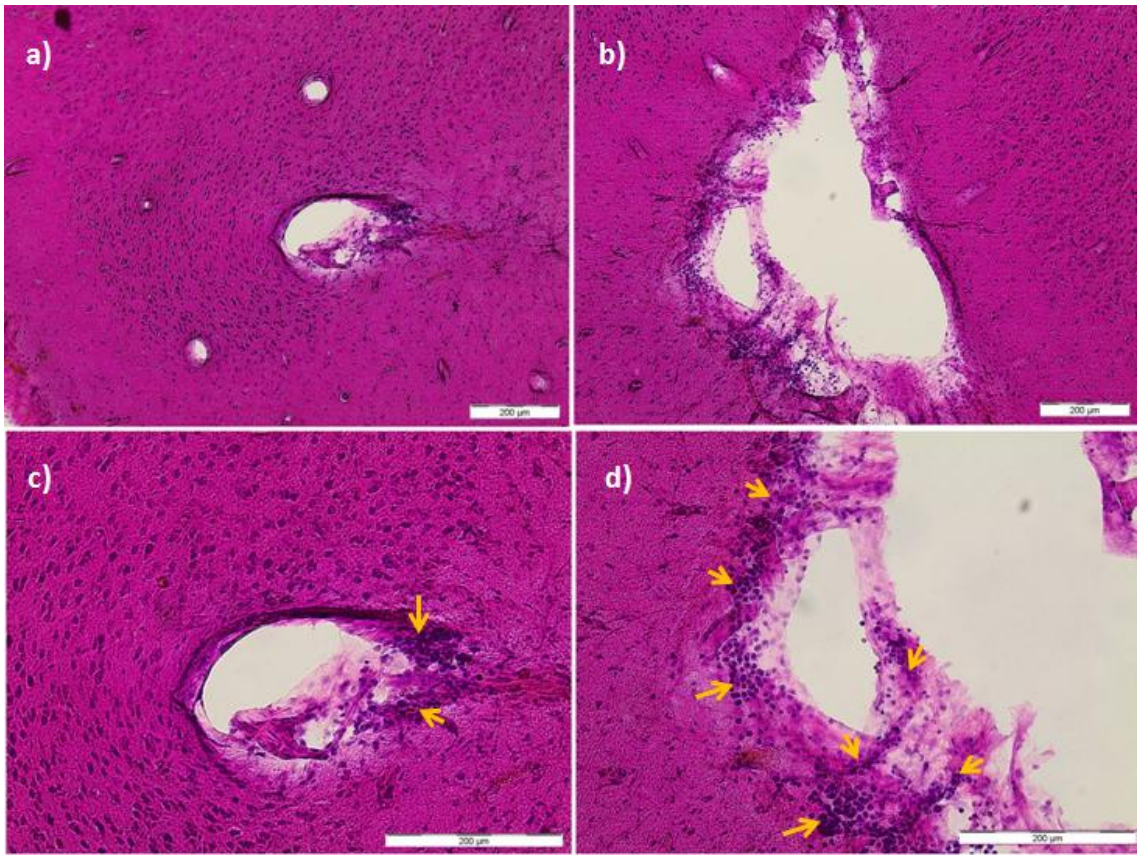

Figure 18 – Chronic inflammatory response. A) and C) - coated probe wound; B) and D) – uncoated probe wound. The bottom images correspond to a 2x zoom of the previous ones, with the signalization of the glial cells such as lymphocytes and plasmocytes.

4. Conclusions and Future Perspectives

This project proposed structural modifications of silicon probes in order to reduce the implants immune inflammatory response, as well as improving the electrical signal recorded from the microelectrodes. For that purpose, a combined coating of chitosan and gold nanoparticles was produced, associated with microelectrodes modifications by galvanostatic electrodeposition of PEDOT/PSS. These structural modifications were studied and tested before a chronic surgery, with the inflammatory response and electrical recording results along and after the surgery being presented also.

A film constituted by five layers of chitosan and gold nanoparticles combined was deposited in silicon microelectrode arrays by dip-coating process. The coating presented great morphological and electrochemical properties pre-surgery, with an increase in average electrodes impedance of 7 kΩ and an average thickness of 50 nm, being also characterized by some roughness and a contact angle of 64.7 º. The gold nanoparticles were distributed along the film, with an average diameter of 16 nm. The PEDOT/PSS electrodes modifications proved to be an efficient and reliable method to diminish the electrodes impedance, reducing it on a scale of some hundreds of kΩ.

To test the coating's behavior in chronic surgery, a three week experiment was performed on a rodent (*Long Evans*). Two probes were implanted, one with only the electrodes modifications using PEDOT/PSS and another one with the Chi/AuNp film coated on top of the modified electrodes. Both probes performances were evaluated in terms of impedance variation, detection and characterization of neuron spikes and histological tests. With an initial average value of 0.122 ± 0.1 MΩ, the electrodes impedances for the uncoated probe at the end of the experiment were of 2.538 ± 0.9 MΩ, reaching values that turn the probe unusable to detect and record neural activity. However, for the coated probe the final impedance value was of 0.735 ± 0.4 MΩ, allowing the recording of numerous spikes and their respective characterization. The coating of Chi/AuNp in conjunction with the electrodes modifications by PEDOT/PSS presents then an efficient solution to improve the silicon probes performance in chronic implants to at least one month.

Spontaneous neuronal activity was detected and recorded by both probes. On the acute recordings, both probes performed well, detecting several and ample neurons spikes (only one electrode was analyzed for both probes, electrode number 22). However, as the experiment ran through, the differences between both probes performance became more apparent, sustained by

the results obtained half-way through and at the conclusion of the experiment, where the uncoated probe was unable to detect any significant neuron spikes (the coated probe continued to detect spikes, with an average amplitude of 281 μV).

A histological characterization of rodents brain cells allowed the detection and visualization of a minor chronic inflammatory response for both probes wounds. Nevertheless, the significantly superior number of glial cells around the uncoated probe wound, when compared with the coated one, suggests that the deposition of the biocompatible film along with the electrodeposition of PEDOT/PSS on the probe reduced the organism immune response.

As for future perspectives, for a deeper study in how the deposition of a biocompatible coating affects the probe's performance in chronic implants, further surgeries need to be prepared regarding the deposition of this five layers film, comparing the results between a coated and an uncoated probe for an extended period of time (4-6 months for example). The variation of the diverse properties of the coating, such as thickness or the solutions concentration, should also be tested, enabling a comparison between the different deposited coatings performance in rodents chronic implants.

For a possible optimal improvement in performance, both electrical and biologically, the encapsulation and incorporation of anti-inflammatory agents (through nanoshells or biodegradable polymers for example) on a biocompatible film may lead to an even further reduction on the organism immune response, as well as to promote the regeneration of nervous system cells.

5. References

[1] S. F. Cogan, "Neural stimulation and recording electrodes.," *Annu. Rev. Biomed. Eng.*, vol. 10, pp. 275–309, Jan. 2008.

[2] R. Mukamel and I. Fried, "Human Intracranial Recordings and Cognitive Neuroscience," *Annu. Rev. Psychol.*, vol. 63, no. 1, pp. 511–537, 2012.

[3] M. Seeck, F. Lazeyras, C. M. Michel, O. Blanke, C. A. Gericke, J. Ives, and J. Delavelle, "Non-invasive epileptic focus localization using EEG-triggered functional MRI and electromagnetic tomography," *Electroencephalography and Clinical Neurophysiology*, vol. 106, pp. 508–512, 1998.

[4] V. S. Polikov, P. a. Tresco, and W. M. Reichert, "Response of brain tissue to chronically implanted neural electrodes," *J. Neurosci. Methods*, vol. 148, no. 1, pp. 1–18, 2005.

[5] R. J. Vetter, J. C. Williams, J. F. Hetke, E. a. Nunamaker, and D. R. Kipke, "Chronic neural recording using silicon-substrate microelectrode arrays implanted in cerebral cortex," *IEEE Trans. Biomed. Eng.*, vol. 51, no. 6, pp. 896–904, 2004.

[6] S. Takeuchi, D. Ziegler, Y. Yoshida, K. Mabuchi, and T. Suzuki, "Parylene flexible neural probes integrated with microfluidic channels.," *Lab Chip*, vol. 5, no. 5, pp. 519–523, 2005.

[7] J. Zhang, F. Laiwalla, J. a Kim, H. Urabe, R. Van Wagenen, Y.-K. Song, B. W. Connors, F. Zhang, K. Deisseroth, and A. V Nurmikko, "Integrated device for optical stimulation and spatiotemporal electrical recording of neural activity in light-sensitized brain tissue.," *J. Neural Eng.*, vol. 6, no. 5, p. 055007, 2009.

[8] J. C. Sanchez, N. Alba, T. Nishida, C. Batich, and P. R. Carney, "Structural modifications in chronic microwire electrodes for cortical neuroprosthetics: A case study," *IEEE Trans. Neural Syst. Rehabil. Eng.*, vol. 14, no. 2, pp. 217–221, 2006.

[9] M. HajjHassan, V. Chodavarapu, and S. Musallam, "NeuroMEMS: Neural Probe Microtechnologies," *Sensors*, vol. 8, no. 10, pp. 6704–6726, Oct. 2008.

[10] B. Y. D. E. Goldman, "IN MEMBRANES (From the Department of] Physiology , College of Physicians and Surgeons , Columbia University , New York) The Journal of General Physiology," pp. 37–60, 1943.

[11] T. F. Chan and J. Shen, "Image processing and analysis: variational, PDE, wavelet, and stochastic methods," *Book*, no. October 2015, p. 400, 2005.

[12] G. Buzsáki, C. a. Anastassiou, and C. Koch, "The origin of extracellular fields and currents — EEG, ECoG, LFP and spikes," *Nat. Rev. Neurosci.*, vol. 13, no. 6, pp. 407–420, 2012.

[13] A. P. Alivisatos, A. M. Andrews, E. S. Boyden, M. Chun, G. M. Church, K. Deisseroth, J. P. Donoghue, S. E. Fraser, O. J. Lippincott-schwartz, L. L. Looger, S. Masmanidis, P. L. Mceuen, A. V Nurmikko, H. Park, D. S. Peterka, C. Reid, M. L. Roukes, A. Scherer, M. Schnitzer, T. J. Sejnowski, K. L. Shepard, D. Tsao, G. Turrigiano, P. S. Weiss, C. Xu, O. O. R. Yuste, and X. Zhuang, "Nanotools for Neuroscience and Brain Activity Mapping," *ACS Nano*, vol. 7, pp. 1850-66, 2013.

[14] F. Franke, D. Jäckel, J. Dragas, J. Müller, M. Radivojevic, D. Bakkum, and A. Hierlemann, "High-density microelectrode array recordings and real-time spike sorting for closed-loop experiments: an emerging technology to study neural plasticity," *Front. Neural Circuits*, vol. 6, no. December, pp. 1–7, 2012.

[15] S. Venkatraman, J. Hendricks, S. Richardson-Burns, E. Jan, D. Martin, and J. M. Carmena, "PEDOT coated microelectrode arrays for chronic neural recording and stimulation," *2009 4th Int. IEEE/EMBS Conf. Neural Eng. NER '09*, vol. 4, pp. 383–386, 2009.

[16] S. J. Wilks, S. M. Richardson-burns, J. L. Hendricks, D. C. Martin, and K. J. Otto, "Poly (3 , 4-ethylenedioxythiophene) as a micro-neural interface material for electrostimulation," *Front Neuroengineering*, vol. 2, no. June, pp. 1–8, 2009.

[17] K. a Ludwig, N. B. Langhals, M. D. Joseph, S. M. Richardson-Burns, J. L. Hendricks, and D. R. Kipke, "Poly(3,4-ethylenedioxythiophene) (PEDOT) polymer coatings facilitate smaller neural recording electrodes.," *J. Neural Eng.*, vol. 8, no. 1, p. 014001, 2011.

[18] W. Franks, I. Schenker, P. Schmutz, and A. Hierlemann, "Impedance characterization and modeling of electrodes for biomedical applications," *IEEE Trans. Biomed. Eng.*, vol. 52, no. 7, pp. 1295–1302, 2005.

[19] R. Biran, D. C. Martin, and P. a Tresco, "Neuronal cell loss accompanies the brain tissue response to chronically implanted silicon microelectrode arrays.," *Exp. Neurol.*, vol. 195, no. 1, pp. 115–26, Sep. 2005.

[20] J. N. Turner, W. Shain, D. H. Szarowski, M. Andersen, S. Martins, M. Isaacson, and H. Craighead, "Cerebral astrocyte response to micromachined silicon implants.," *Exp. Neurol.*, vol. 156, no. 1, pp. 33–49, 1999.

[21] K. E. Crompton, J. D. Goud, R. V. Bellamkonda, T. R. Gengenbach, D. I. Finkelstein, M. K. Horne, and J. S. Forsythe, "Polylysine-functionalised thermoresponsive chitosan hydrogel for neural tissue engineering," *Biomaterials*, 2007. [Online]. Available: https://neurolab.gatech.edu/wp-content/uploads/bellamkonda/publications/2007-01_crompton_goud_bellamkonda_gengenbach_finkelstein_horne_forsythe.pdf. [Accessed: 16-Feb-2015].

[22] H. Yang, S. Zhou, and X. Deng, "Preparation and Properties of Hydrophilic – Hydrophobic Chitosan Derivatives," *Journal of Applied Polymer*, no. May, pp. 1625–1632, 2004.

[23] J. D. Bumgardner, R. Wiser, S. H. Elder, R. Jouett, Y. Yang, and J. L. Ong, "Contact angle, protein adsorption and osteoblast precursor cell attachment to

chitosan coatings bonded to titanium.," *J. Biomater. Sci. Polym. Ed.*, vol. 14, no. 12, pp. 1401–1409, 2003.

[24] E. E. Connor, J. Mwamuka, A. Gole, C. J. Murphy, and M. D. Wyatt, "Gold Nanoparticles Are Taken Up by Human Cells but Do Not Cause Acute Cytotoxicity," *Small*, vol. 1, no. 3, pp. 325–327, 2005.

[25] S. Rose, A. Prevoteau, P. Elzière, D. Hourdet, A. Marcellan, and L. Leibler, "Nanoparticle solutions as adhesives for gels and biological tissues.," *Nature*, vol. 505, no. 7483, pp. 382–5, 2014.

[26] J. Kimling, M. Maier, V. Okenve, V. Kotaidis, H. Ballot, a Plech, and B. Okenve, "Turkevitch method for gold nanoparticle synthesis revisited," *J. Phys. Chem. B*, vol. 110, no. 95 mL, pp. 15700–15707, 2006.

[27] M. P. Ward, P. Rajdev, C. Ellison, and P. P. Irazoqui, "Toward a comparison of microelectrodes for acute and chronic recordings," *Brain Res.*, vol. 1282, pp. 183–200, 2009.